PERIODICA POLYTECHNICA SER. CIVIL ENG. VOL. 35, NOS. 3-4, PP. 243-264 (1991)

LOAD TEST OF THE TRUSSED RIVER STRUCTURE OF THE RAILWAY BRIDGE OVER THE TISZA BETWEEN CSONGRÁD AND SZENTES

P. TOMKA, M. IVÁNYI and M. KÁLLÓ

Department of Steel Structures
Technical University of Budapest

Received: September 1, 1992

Abstract

In this paper, the railway bridge of the longest span ever built in Hungary is dealt with. It contains also information on the structures constructed prior to this recent one. The behaviour of the new trussed structure is discussed in detail. The phenomena not traceable by traditional calculation were revealed by measurements destined and performed to clear up the numerous problems of the detail. In the paper, the secondary stresses of joints playing an especially active role with respect to fatigue-life as well as the complex holding character of the individual structural elements, the deflections of basic importance for the classification of bridges, the possible consequences of the applied layout of the upper sway-bracing and the effect of dynamic load are dealt with in detail. In the course of evaluation, simply treatable computational models are also described here, the results of which are compared with the concrete, measured values.

Keywords: railway bridge, experimental, secondary stress, floor structure, sway-bracing, dynamic.

Introduction

The construction of the permanent bridge between Csongrád and Szentes started in 1901, and it was opened to traffic on 3 December, 1903.

The riveted bridge made of steel cast was a trussed girder of nine openings as a series of simply supported elements. The flood area structure – with one span on the Csongrád side, and with five spans on the Szentes side – was a half-trough trussed structure of parallel chords, while the section of the three intermediate spans contained trough structures of truncated segmental truss.

The middle part of the river bridge over the stream was the most impressive one with its span of nearly 120 m long. No railway bridge with a span exceeding this one has ever been built in Hungary.

Late 1944, the river bed structure of 120 m span and the adjacent structure on the Csongrád side were blown up. The bridge reconstructed under adverse circumstances was opened to traffic on 15 December, 1946.

The flood area span, as well as the extreme river spans of the reconstructed bridge remained unchanged. The blown up middle structure of 120 m long was damaged to such an extent that it could not be reconstructed any more, and as a result, this span was divided into two parts with the help of a new pier. Into the Szentes side part of the two span section laid out as described, the riveted structure of the demolished bridge over the river Maros at Magyarcsanád was transferred and inserted, while into the other part of it, a bolted bridge structure of Roth–Wagner type was built in. On these bridge sections, the covering of the wagon way was made of hardwood plank.

Up to 5 November, 1981 – which was the date of the opening to traffic of the highway bridge –, highway and railway traffic of alternating direction was maintained.

On the basis of the previous technical and economic examinations, the miantenance of the railway traffic also during the construction was an important viewpoint with constructional designs. This requirement could be met economically in a way that the new bridge was erected close to the old one, at 10 metres downstream the Tisza with a minimal correction of alignment as built on new masonry.

In *Fig. 1*, the span layout of the bridge in service between 1946 and 1987, as well as the layout of spans of the bridge opened to traffic in 1987 are illustrated.

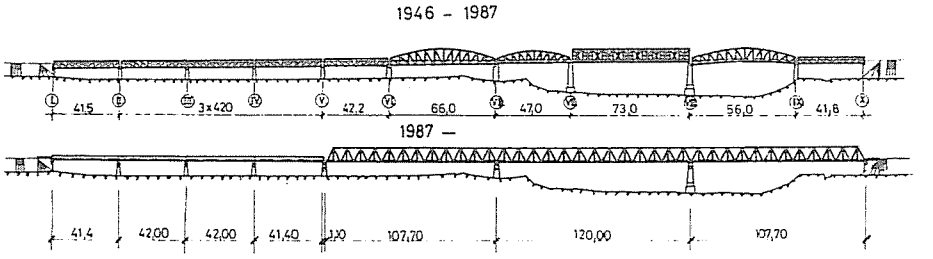

Fig. 1. General view of the bridge

For the sake of omitting the extensive scaffold erection operations, the assemblage of the superstructure on the river banks, and its subsequent push-in was considered as the most economical assemblage method of construction.

This method of assemblage required the design of continuous, multispan main girders. As a result, the river bridge was built as a trussed

structure of trough type with the following span lengths: 107.7 + 120.0 + 107.7 m, while the flood area structure on the Szentes side was a trough-type plate girder structure with spans of 41.4 + 42.0 + 42.0 + 41.4 m.

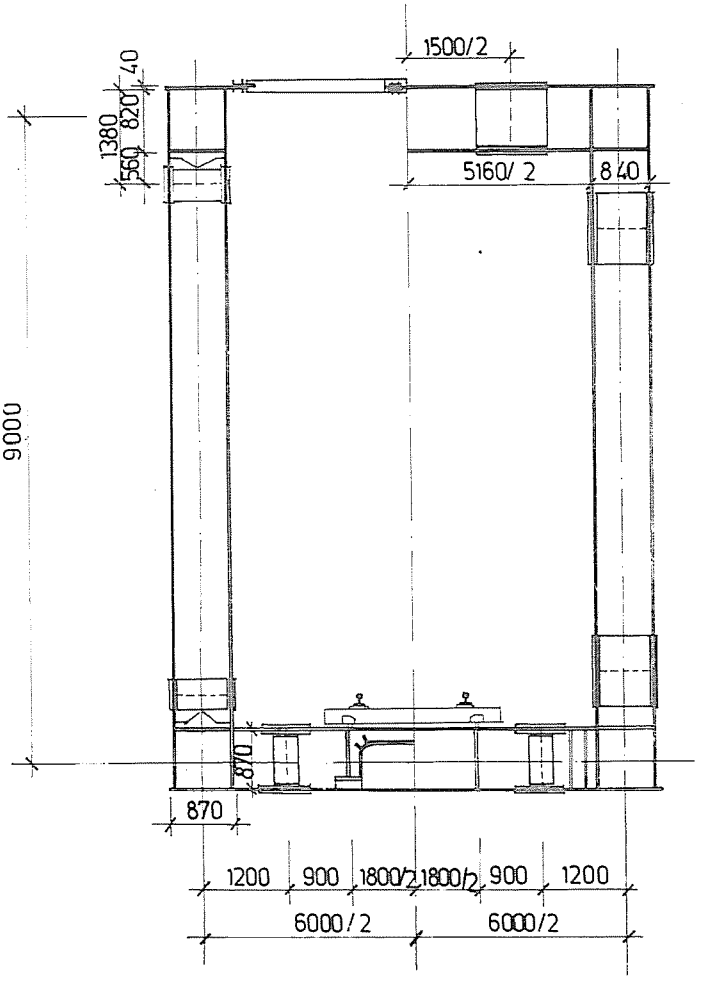

Fig. 2. Cross-sections of the river-bridge

The span layout of the trussed bridge deviating from the old one has the following advantages:

- omission of three piers (VI, VIIa and IX), which is worthwhile with respect to flood control and protection, too,
- the span ratio of the three-span continuous structure is more favourable (1:1, 1:1),

- there is no need of anchorage at the extreme supports,
- on the Csongrád side, the push-in operation can be performed starting from the assemblage field all along, so there is no need of inserting another structure of a different system with a span of 42 m.

The use of wooden sleepers on the floor structure is determined by the fact that in the case of a speed of 100 km/h reckoned with for the line, the direct rail fastening is no more advisable, and the application of a ballast bed is not economical due to its heavy weight, and it is not verified by speed either. The total length of the river bridge is 336.4 m. The distance between the mains is 6000 mm, while that between the stringers is 1800 mm. The chords of the main Warren truss are parallel with each other. The cross-sectional layout of the river bridge is shown in *Fig. 2*. The chords are closed profiles with four walls, while the diagonals are open I-profiles. The profile of the hanger connected to every second floor beam is also of I-shaped profile (*Fig. 3*).

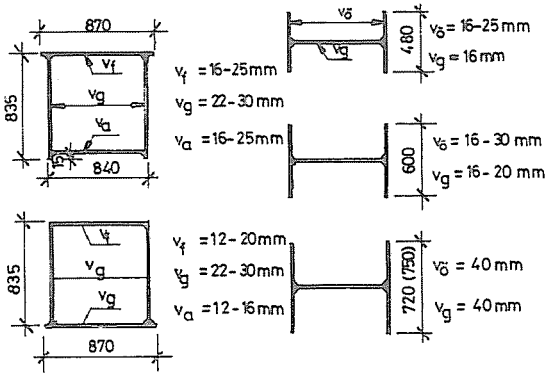

Fig. 3. Cross-sections of chords and diagonals

Typical structural details are shown in *Figs. 4* and *5*. At the main joint of the lower chord – where the diagonals are connected to – 3-3 diaphragms are inserted so that at these places the bridge can be supported during the assemblage, and be lifted out by jacks.

Between the chords of the mains, the horizontal forces are taken by the bottom and upper sway-braces.

The layout of the floor structure can be seen in *Figs. 6* and *7*. It is an interesting feature of it that there is no sway-bracing between the two stringers in spite of their relatively great length, instead the stringers form a Vierendeel truss with the transverse braces. This solution was permitted by the fact that the floor structure was oversized because of the fatigue.

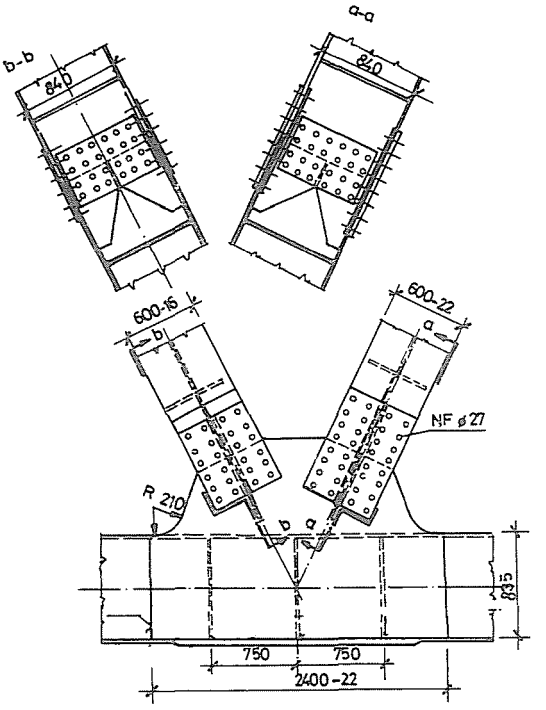

Fig. 4. Main joint of the lower cord

Generally, four floor beams and a four-span distance of the stringer formed one manufacturing unit with welded joints.

The butts of the stringers are connected to each other and to the knee-brace of floor beams by bolted connections. The breaks in the stringers are destined to prevent the contribution between the floor structure and the mains.

Fig. 8 shows the entire trussed bridge structure during the assemblage.

The load test of the river bridge was carried out by the Department of Steel Structures at the Technical University of Budapest between 27 and 30 November, 1986. Here, we should like to describe the most interesting results achieved through the detailed analysis of, and the comparison between the experimental data measured by a great number of sensors, as well as the calculations associated with the structure, and the copious experience gained in this field.

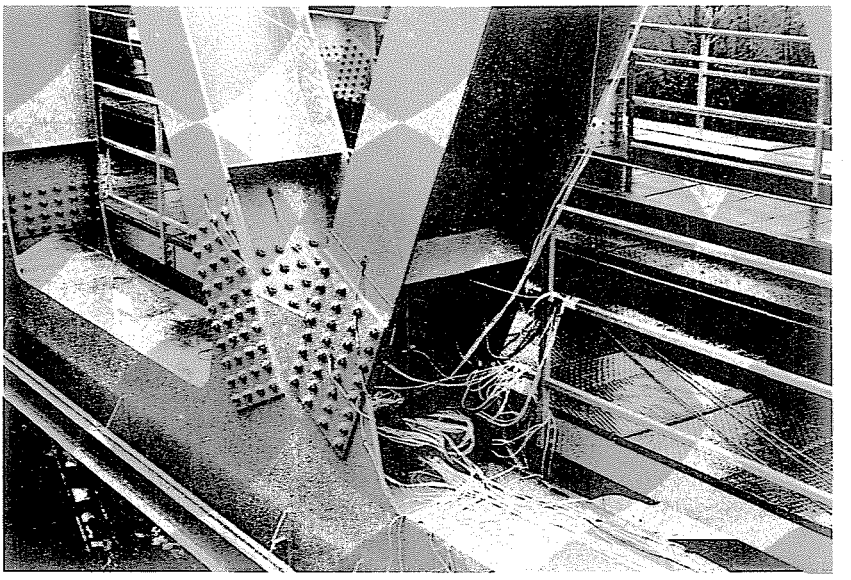

Fig. 5. Photo of a main joint of the lower chord

Secondary Stresses at the Joints

In the traditional calculation of the trussed girders, ideal hinges were assumed at the joints. With loads reduced to the joints, the girder is dealt with as a separate structure. The result of the approximate calculation outlined in the foregoing is a concentric bar force, or a uniformly distributed normal stress, respectively.

At the design for static load, the deviation of the actual structure from the computational model is taken into consideration by the design systems with the use of traditional rules. The case is more complicated when designing for cyclically repeated load (fatigue) is in question. In this case, the load-carrying capacity of the structural elements depends – to a greater extent – on the non-uniform stress distribution. The procedure given in the Hungarian prescriptions – according to which the normal stresses calculated from the service value of the vehicle load should be increased by a constant value (20 MPa) in the case of welded joints – can not be considered a definite solution.

The actual stress distribution is more complex, which can be approximated much better by a computational model reckoning also with the structural details of the main girder and the contribution among the main and other structural elements (floor structure). From among the factors

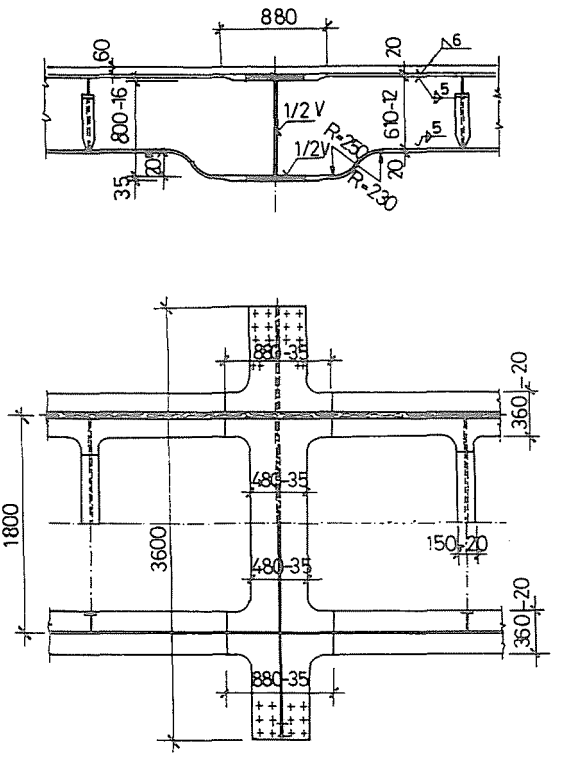

Fig. 6. Layout of the floor structure

influencing the actual stress distribution, the following ones should be underlined.

The joints of the main girder can be really considered to be moment-resistant. In this way, bending moment (M_x) of the vector perpendicular to the plane of the girder will arise in the bars.

The floor beam connected to the main girder by partial restraint, as well as the verticals and diagonals of the main girders form a U-shape frame in the case of a bridge with open cross-section while they form a closed frame in the case of a layout with upper sway-bracing. In this latter one, the load applied to the axes will give rise to bending moment (M_y) with a vector parallel to the longitudinal axis of the main girder. This will cause a torsion in the chords, while it will transmit a compression force to the upper sway-bracing.

The diagonals and verticals are generally connected into the gusset plates parallel to the plane of the main girder. To this fact can be con-

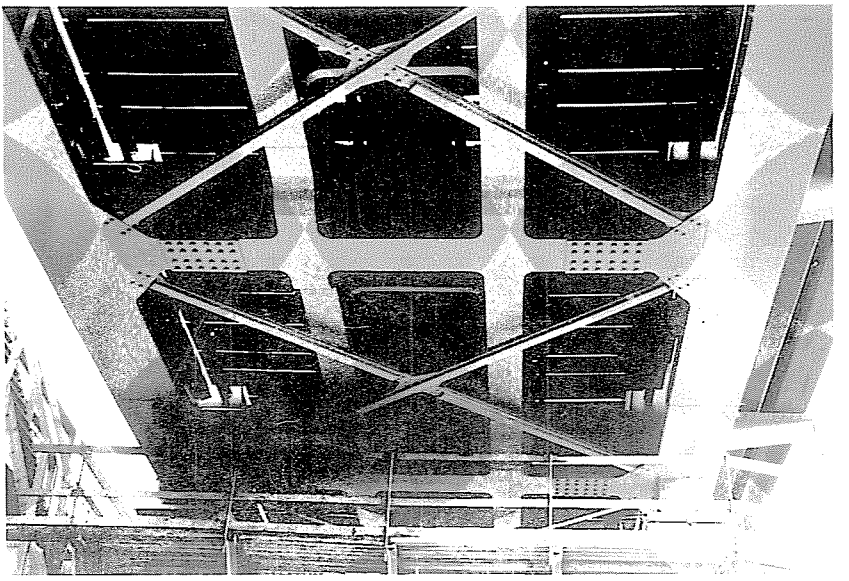

Fig. 7. Photo of the floor structure

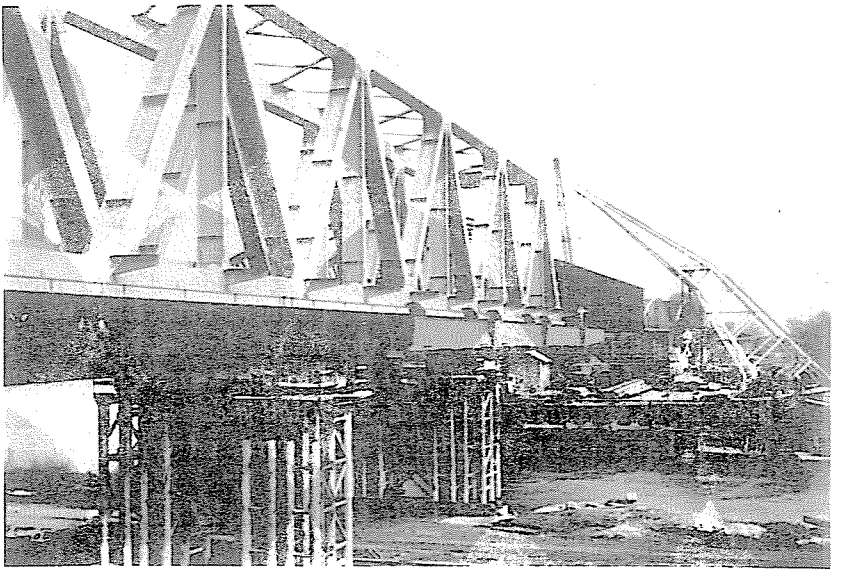

Fig. 8. The entire trussed bridge structure during assemblage

tributed that the value of stresses in the elements (flanges) of the bars in question will be increased to a considerable extent in the vicinity of the connection. This effect is even stronger if the webs of the diagonals are not connected.

The floor structure with its supporting or stiffening structural elements, as well as the sway-bracings of the main girder form a complex spatial structure having a complex holding effect with the main girder. The difficulty of calculations is farther increased by the fact that the connection of the individual components is a partial restraint, but the measure of restraint can hardly be approximated, or only with a rough estimation. The mentioned complex holding effect generally reduces the stresses of the main girder.

Neither can the effect of eccentricity be neglected. In most cases, the design layout is already eccentric even though only to a small extent. But the inaccuracies resulted from the manufacture and assemblage deficiencies are essentially greater.

It follows from the analysis given above that even a calculation much more complex than the traditional one can follow the actual behaviour of the structure with a due accuracy. Therefore, the data measured on the structure are of fundamental significance.

In *Fig. 9*, the stresses measured in the cross-sections of the diagonal with I-profile are shown. The distribution of stresses arisen in the cross-sectional areas immediately before their connection shows well the normal stresses corresponding mainly to bending moments M_x and M_y.

The stresses measured in the cover plates at the connection show the additional fact that webs take only a relatively small force. By integrating the measured stresses, the diagram representing the variation of the forces acting on the web and flanges, or the cover plates joining those along the axis of the bar (on the right-hand side of the Figure) clearly shows that the force is transferred, first of all, through the flanges.

The equation of the plane stretching on the measured stresses was also calculated. The result of the three-parameter regression determined by the method of the least squares will be a function of the following form:

$$\sigma_{x,y} = \sigma_N + \xi\sigma_x + \eta\sigma_y$$

where:

$\sigma_{(x,y)}$	the value of stress at point with x and y coordinates, resp., of the cross-sectional area,
σ_N	the average stress,
σ_x	the absolute value of the normal stress corresponding to bending moment M_x in

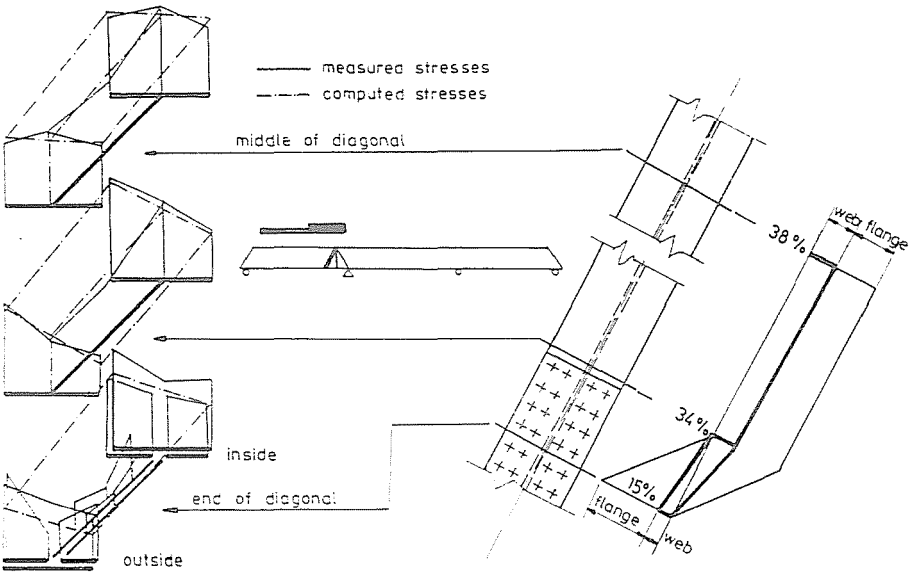

Fig. 9. Stress pattern in the tensile diagonal

the extreme fibre, while

σ_y that corresponding to M_y,

$\xi = \frac{x}{x_{\max}}$,

$\eta = \frac{y}{y_{\max}}$,

$x_{\max}, y_{\max}$ are the extreme fibre distances.

The values of the above stress components arisen by the effect of the load changing gradually its position along the bridge are shown in *Fig.10.*

The maximum deviations from the average value, which is also called the secondary stress of the joints, can be determined by the expression:

$$\sigma_{\max} = \max\ [\ \mathrm{abs}\{\sigma_{\mathrm{meas}} - \sigma_N\}].$$

This value, too, was indicated in the Figure. Omitting the detailed analysis of the results, it can be stated that under the influence of a load approximately corresponding to the service load, the maximum value of the secondary stresses of the joints will be about 20 MPa. In the case of another diagonal, this value was yielded as 24 MPa, i.e. it exceeded the specified value mentioned above.

In *Figs. 11* and 12, the secondary stresses measured in the joints of the lower and upper chord, respectively, are shown. In these cases, the value of σ_y is obviously zero. In the case of both chords, the value of $\sigma_{\max}$

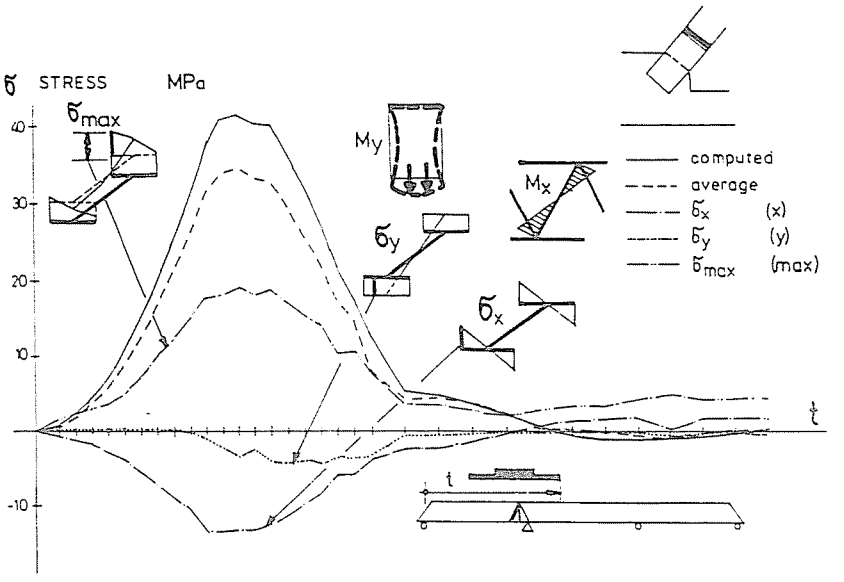

Fig. 10. Secondary stresses at the gusset plate of a tensile diagonal

is essentially smaller than that measured in the diagonal. In *Fig.11*, the normal stress calculated with the help of the traditional model was also indicated. From the remarkable deviation of the measured and calculated values, the contribution between the lower chord and the floor structure can be followed well.

Contribution between the Main Girder and Floor Structure

The complex holding structure consisting of the stringers and floor beams, as well as the lower chords of the main girder can be calculated also by approximate method. In the following, the results of such a calculation are compared to those measured on the structure.

The principle of the calculation applied here can be seen in *Fig.13*. Its essence is that the total structure is substituted by a section between the two joints. The connection of the stringers and floor beams is assumed as a freely rotating one. The bending moments are calculated from elongation of the bottom chord of the main girder.

The normal stresses arisen in one of the cross-sectional areas adjacent to the disconnection in the stringer as measured and calculated by the above model are indicated in *Fig.13*. It can be clearly seen that the characters of the measured and calculated curves are similar to each other. The

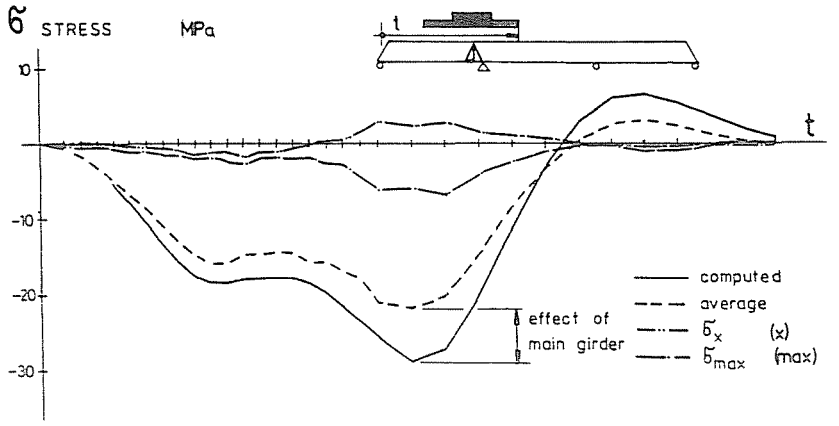

Fig. 11. Secondary stresses in the joints of the lower chord

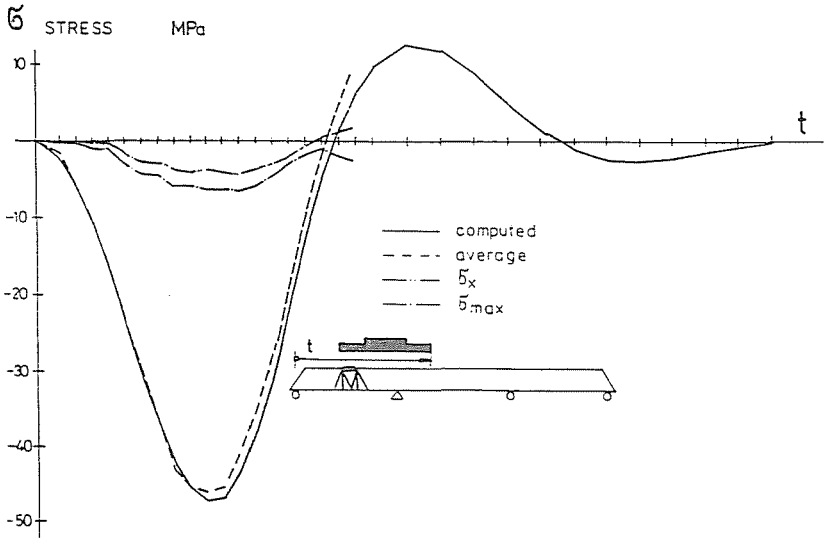

Fig. 12. Secondary stresses in the joints of the upper chord

calculated values are obviously greater to a considerable extent because the connection of the floor beam and the main girder is a partially restrained one deviating from that assumed to be with the calculation.

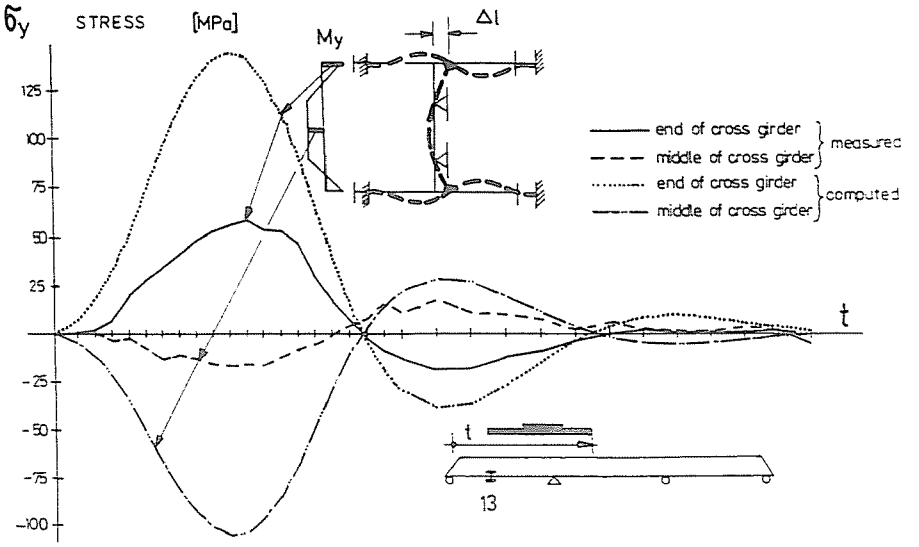

Fig. 13. Normal stresses in the cross girder No. 13.

The stresses arisen in the stringers connected to the above floor beam are shown in *Fig.14*. As it can be seen from the schemes shown in the Figure, the connection of the floor beam and the main girder is assumed a freely rotating one in one case, while a clamped one in the other case.

The uniformly distributed normal stress measured in the stringer falls between the values determined by the two types of calculation, which – in turn – indicates again the fact of a partial restraint.

From the analysis of the two Figures, it can be concluded that – in the given case – the value of the actual stresses will approximately be equal to the mean value given by the calculations assuming a freely rotating and a fully restrained connection of the floor beam.

Deflections

Fig.15 shows the measured deflections caused by the effect of the load changing gradually its position, and those calculated with the use of the hinged model of the main girder. The measured values reached 75–80 % of those calculated. This fully agrees with the experience gained with bridge structures of a similar layout. Its reason is obviously the rigidity of joints

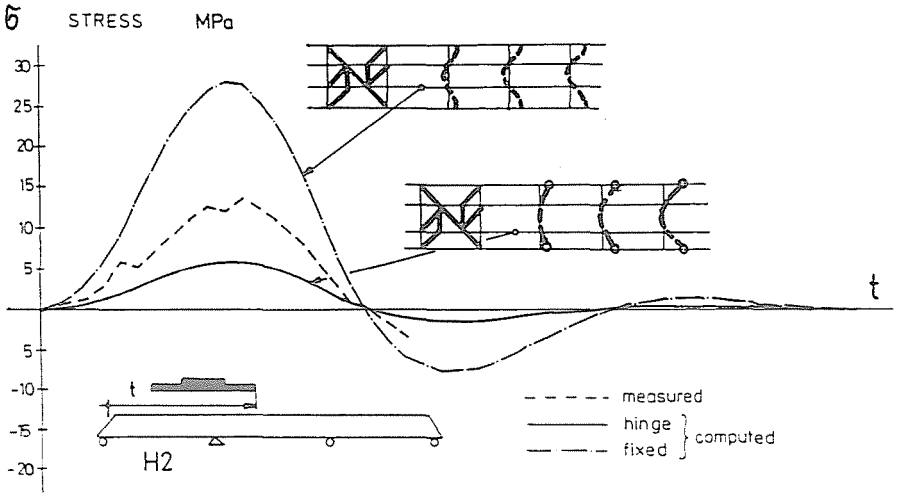

Fig. 14. Normal stresses in the stringer No. H2

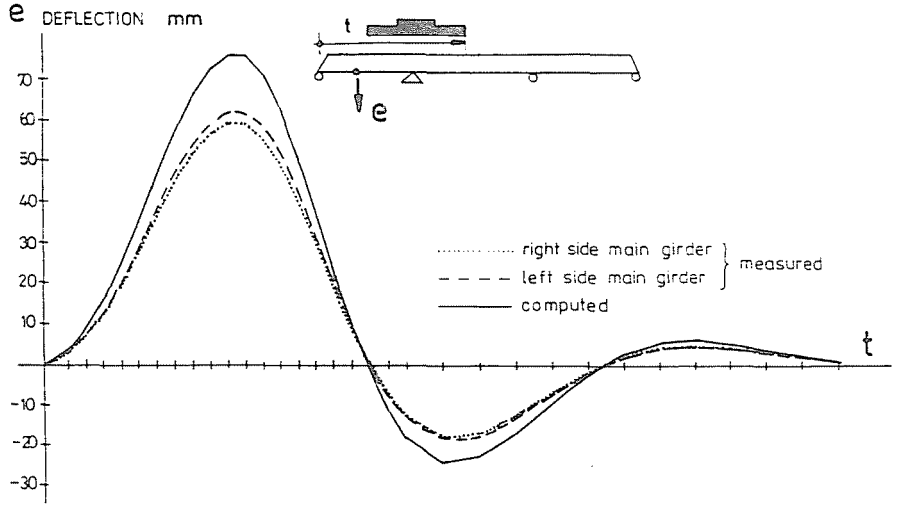

Fig. 15. Deflections of the main girder

analysed in the previous points, and the contribution between the main girder and the floor structure.

Effect of the Structural Layout on the Behaviour of Sway-braces

The joint of the upper sway-bracing applied with the trussed bridge structures at the connection to the main girder and its intermediate joint, respectively, are shown in *Fig. 16.*

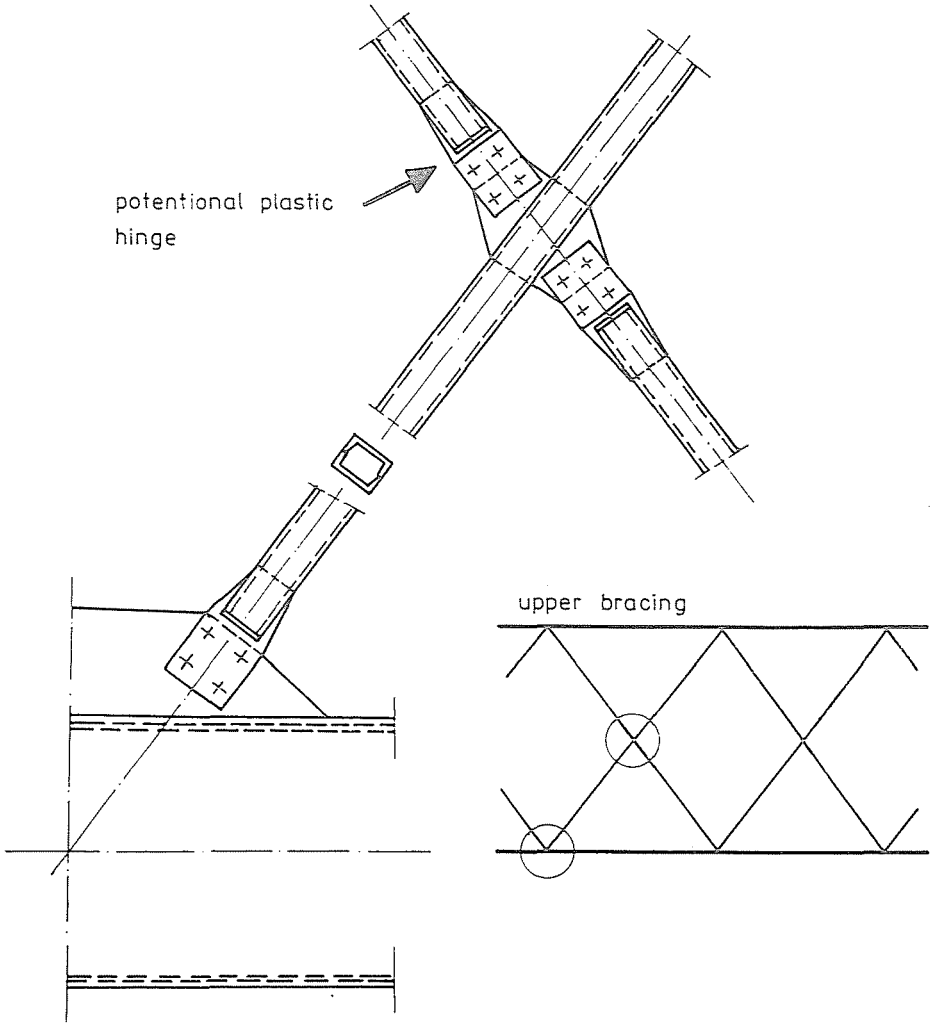

Fig. 16. Layout of the upper bracing

The layout of the detail indicated by arrows is especially unfavourable at the places where the load-carrying capacity of the gusset plate against

bending is drastically decreased in comparison to that of diagonal while the value of the bending moment is nearly equal to the maximum. When analysing the sway-bracing, two details are dealt with:

- calculation of the bar forces,
- determination of the stresses arisen in the structure by a second-order method.

From among the loads and effects acting on the upper sway-bracing, the most important ones are the following:

- wind load,
- eccentricity of the upper chord of the main girder,
- temperature difference,
- elongation of the upper chord of the main girder, as well as the effect of the frame formed by the verticals, and the upper sway-bracing (in one, the effects yielding by contribution among the main girder with the other structural elements),
- inaccuracies in the manufacturing and assemblage: inaccuracy in the length and shape of the sway-bracing members, the height difference of the main girders,
- eccentricity of the sway-bracing members (joints in single shear or in single friction).

According to the prescription holding at the time of design, the upper sway-bracing should be designed for wind load and a fictitious shear force, the safety factor is 1.2. In the case of a sway-bracing laid out structurally in a proper way, this design concept results in a sway-bracing of adequate load-carrying capacity. However, in the present case, the individual effects were analysed one by one, too.

The static scheme (nodal points) of the sway-bracing was assumed in two ways:

a) fixed and
b) hinged connections of joints.

On the basis of our detailed calculation, we came to the conclusion that the results of the calculations obtained using two kinds of the model did not deviate essentially from each other with the exception of one effect. This effect is the inaccuracy in the length of the diagonals.

In *Fig. 17*, the bar forces are shown which arise if the manufacturing inaccuracy (lack of fitness) of the intermediate sway-bracing members is equal to + 1 mm. The bar force calculated with the use of a rigid model is nearly ten times as much as that calculated using a hinged model. The reason for it is obviously the fact that the flexural rigidity of the upper chord functioning as the chord of the sway-bracing exceeds essentially that of the sway-bracing members. As an illustration of the results, in the lower

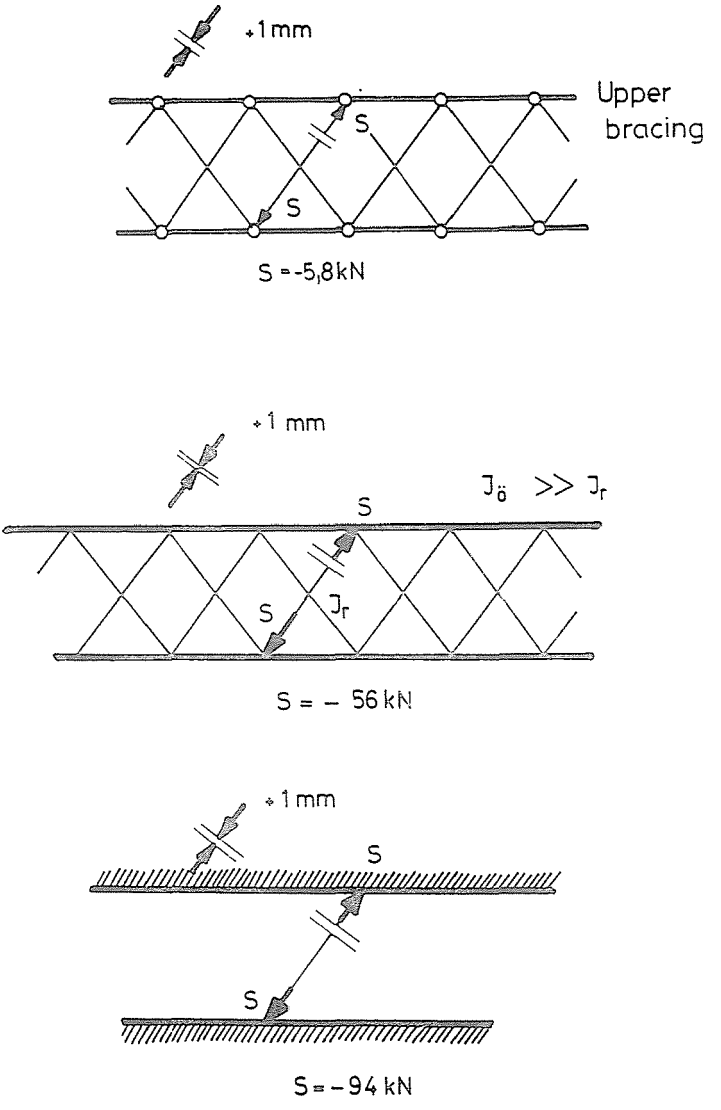

Fig. 17. Bar forces in the diagonals from lack of fitness

part of the Figure the compression force which arises in the diagonal forced into between the two rigid end plates is also represented.

The calculation of normal stresses is shown in *Fig. 18.* By rotating in the plane the intersection sway-bracing members, a planar bar structure consisting of bars of varying cross-sectional area will be obtained. Loading effects are:

- manufacturing inaccuracy in the length of both intersecting diagonals of + 2 mm,
- crookedness of 6 mm in the middle,
- weight of the sway-bracing,

i.e. the loads and effects largely correspond to the state of assemblage.

In the following part of the Figure, the bending moment diagram of the intersected diagonal as determined by a second-order method can be seen, while in the lower part of the Figure, the diagram of normal stresses calculated with the use of the actual cross-sectional characteristics is represented. It can be clearly seen that at the critical places where the cross-sectional area is formed only by the gusset plate welded to the U-profile, the value of the normal stress will increase abruptly. With the assumption of a perfectly elastic material, the value of the normal stress arisen in these cross-sectional areas exceeds considerably the nominal value of the yield stress. As a matter of fact, a yield mechanism is developed together with the corresponding residual deformations perpendicular to the plane of the bracing. As a consequence, the load-carrying capacity of the sway-bracing itself will be reduced, on the one hand, maybe in such a measure that even the fundamental functions cannot be fulfilled. However, at the same time, the sway-bracing damaged in this way cannot ensure the lateral support of the chords of the main girder, either, and this – in turn – involves a reduction in the load-carrying capacity of the main girder as well.

The calculation detailed above accounts of the fact that certain individual panels of the upper sway-bracing underwent a damage identical with the calculated one in the course of assemblage. The lesson learnt from those said above is that in the course of design the rule should not be disregarded that the connection of the sway-bracing members should be laid out fully identically with respect of load-carrying capacity. It should also be noted that the behaviour of the quadrangular trussing is more advantageous in every respect.

Examination of the Effect of Dynamic Load

For the sake of the dynamic characterization of the bridge, the natural frequencies were also measured. The first natural bending frequency was 1.75 Hz (on the basis of a computer analysis and an averaged power spectrum),

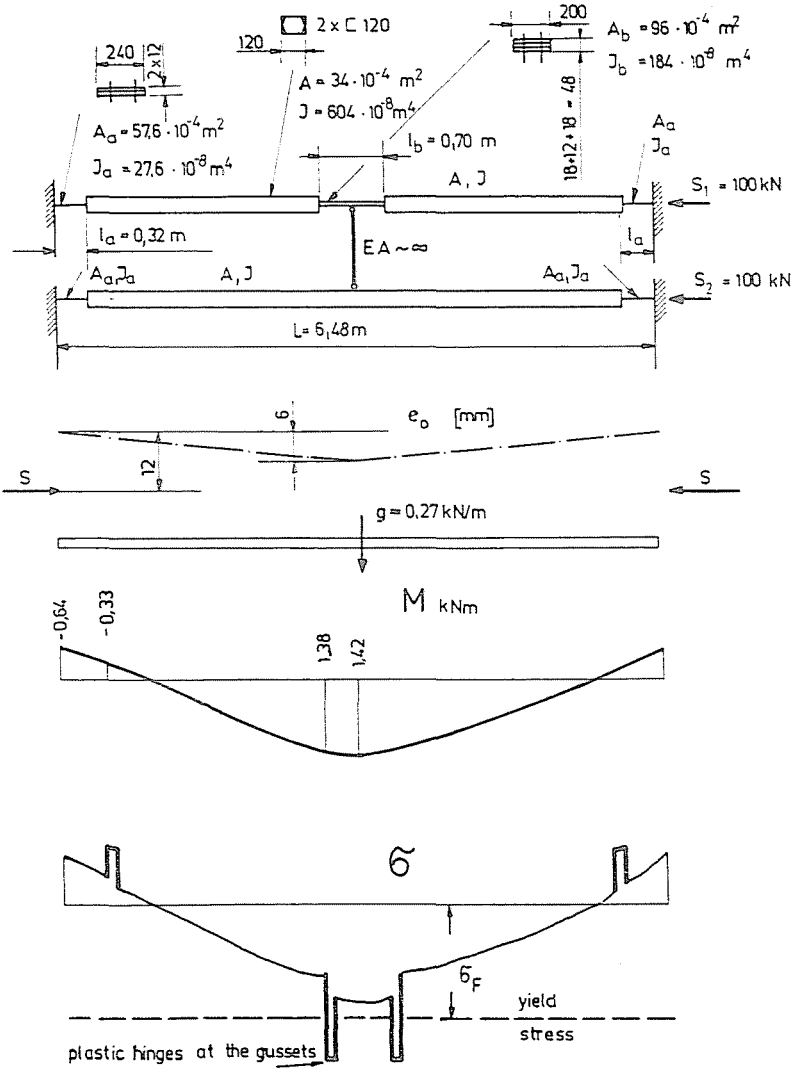

Fig. 18. Second order analysis of the upper bracing

while the second natural bending frequency was 2.7 Hz (*Fig. 19*). The value of the first horizontal natural bending frequency – on the basis of the evaluation of the time functions of the lateral displacements – was 1.1 Hz.

It is interesting to note that this component can be seen – though only with a slight emphasis – in the power spectra shown in *Fig. 18*, too. This fact warns us that – in the case of stochastic excitations – a special care should be taken of the separation of the individual natural frequencies and natural shapes.

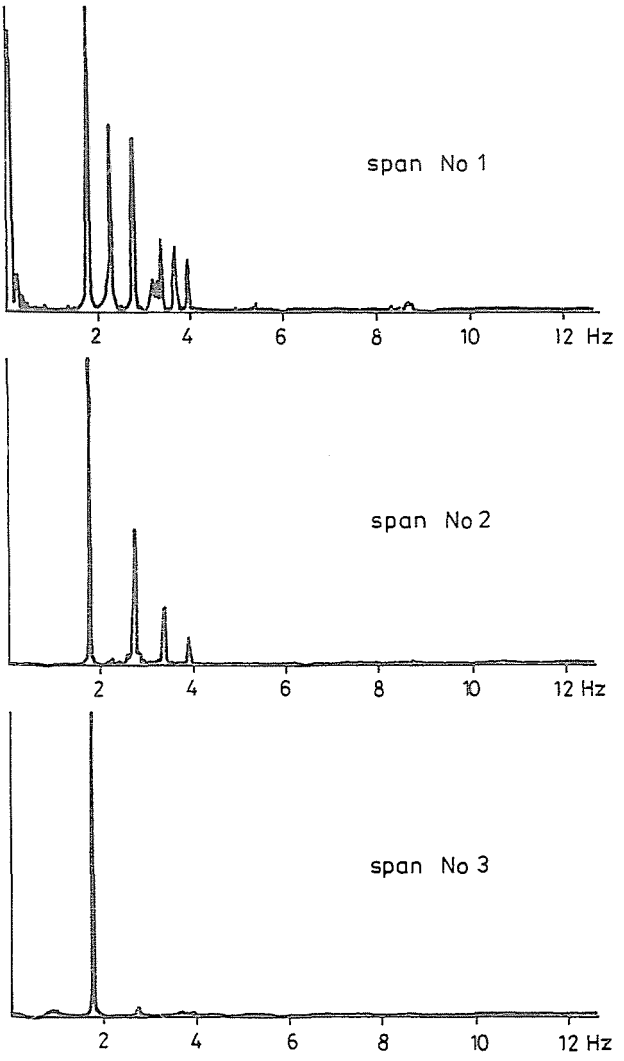

Fig. 19. The natural frequencies of the bridge

The horizontal, transverse displacement of the structure can occur, in principle, only by the effect of the lateral forces arisen during the passing of moving vehicles. This value – according to the Railway Bridge Regulations – can not exceed a fraction of 1/5000 of the span. The value measured in practice during the passing of 2 engines with a mass of 120 t each at a speed of 60 km/h reached only somewhat more than 25 % of that value.

The measured values of deflection verified the results of static measurements. A dynamic effect of 2–5 % could be pointed out on the deflection-time functions. In *Fig. 20*, the deflection and the lateral swaying occurred in the middle span are represented.

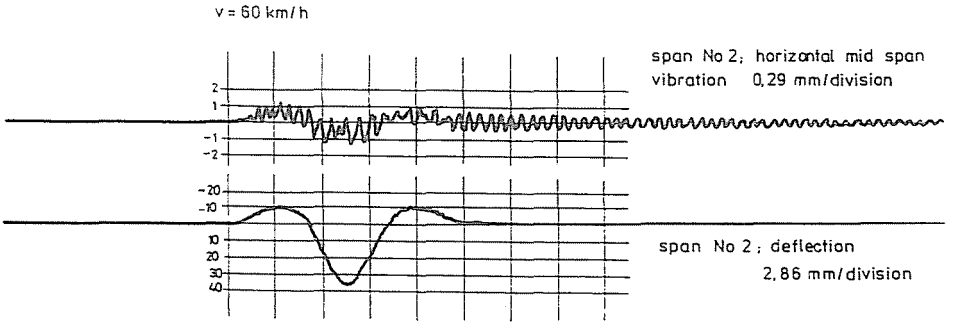

Fig. 20. Deflections and horizontal midspan vibrations

The maximum values of the dynamic coefficient obtained from the stress-time functions as measured on the individual elements are the following:

on the main girder	1.04
on the stringer	1.09
at the restraints of the stringer	1.2

No effect of the considerable compression stress mentioned in the previous point as taken on the elements of the upper sway-bracing involved in the measurements could be detected – which served as a proof of the fact that the experienced permanent deformations could be attributed to the manufacturing inaccuracies of the individual bars.

Otherwise, on the sway-braces, a dynamic coefficient of about 1.5 could be measured with a peak stress of max. 10 MPa. In *Fig. 21*, a stress-time function fixed on the bottom and upper fibres of the sway-bracing's gusset plate is represented, on which the anti-phase components show clearly the bending oscillations in the course of the passing of vehicles.

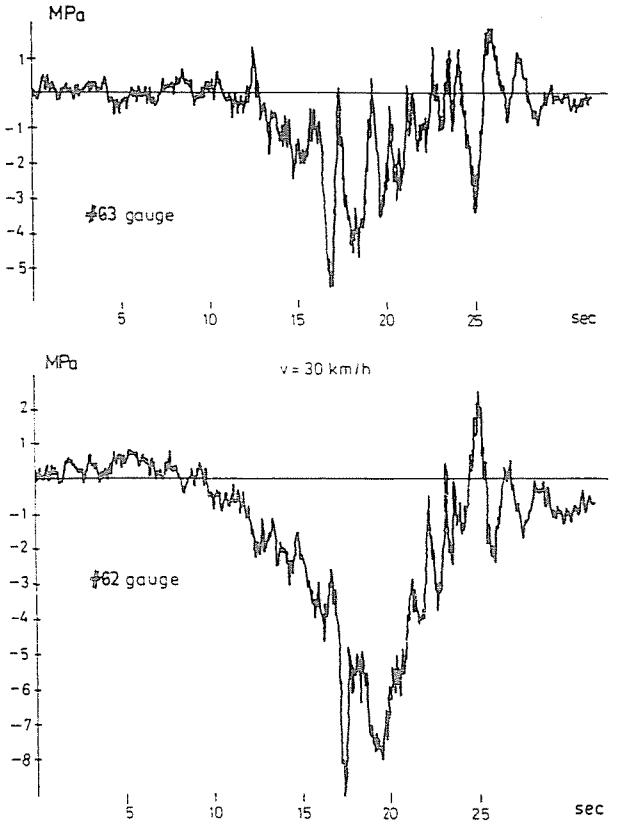

Fig. 21. Stress-time function on the bottom and upper fibres of the sway bracing's-gusset plate

Address:

Dr Pál TOMKA,
Dr Miklós IVÁNYI
Dr Miklós KÁLLÓ
Department of Steel Structures
Technical University,
H-1521 Budapest, Hungary